Application Note - Forensics 2

Depth scans on car paint samples with Raman spectroscopy and LIBS

Lutz Pfeifer, Saskia Damaske, Wolfgang Werncke and Virginia Merk
LTB Lasertechnik Berlin

Introduction

The combination of Raman spectroscopy with laser-induced breakdown spectroscopy (LIBS) has the advantage of coupling two complementary analytical methods: with LIBS it is possible to obtain information about the elemental composition of a sample at the examination point, while Raman spectroscopy reveals the molecular, crystalline or mineralogical structure. Another benefit of combining Raman/LIBS measurements is the opportunity to achieve depth information. Namely, characterization of a sample's constitution when penetrating the surface with repeated laser ablations at the same point. This specific advantage of LIBS or Raman/LIBS experiments has already been extensively demonstrated for thin films with thicknesses ranging from 1 µm up to 30 µm, with examples including the analysis of aluminum layers on steel [1], the stratigraphic investigation of paint layers [2] and for polymer-coated metals [3].

The aim of this technical paper is to demonstrate the suitability of the CORALIS instrument for depth profiling of forensic samples. Here we focus on investigation of a car paint sample consisting of several different layers with an overall thickness of 250 µm.

Instrument

Measurements were done with the CORALIS instrument -- a device capable of performing Raman or LIBS measurements on a single or on a multitude of sampling points. The CORALIS is also capable of acquiring consecutive Raman and LIBS spectra and to do this during depth scans of specified sampling points.

The CORALIS contains a pulsed Nd:YAG laser (1064 nm) for LIBS with variable laser energy and two continuously operating lasers for Raman (532 and 785 nm). The spot diameter of the laser focus on the sample is appr. 10 µm for Raman and 20 µm for LIBS.

The analysis of Raman spectra can be performed with the integrated peak finding algorithm, or via spectral comparison using a comprehensive database (KnowItAll®, Bio-Rad, USA). Furthermore, various baseline correction methods are also integrated into the software and can be applied to the spectra. For the analysis of LIBS spectra, the software provides an element finding algorithm, spectral classification with PCA and PLS-DA, and multivariate quantification methods.

Material and Methods

Investigation samples – in this case, paint flecks – were collected on the street from the remnants of auto accidents. The samples were used as found without any further treatment (e.g. cleaning, grinding or polishing). An example is shown in Figure 1. This sample was fixed onto a piece of poly-crystalline silicon in order to determine the point at which the LIBS laser breaks through. Using consecutive Raman and LIBS measurements and ablations, the characteristic Raman band of Si at 521 cm^{-1} should appear as soon as the sample is fully penetrated.

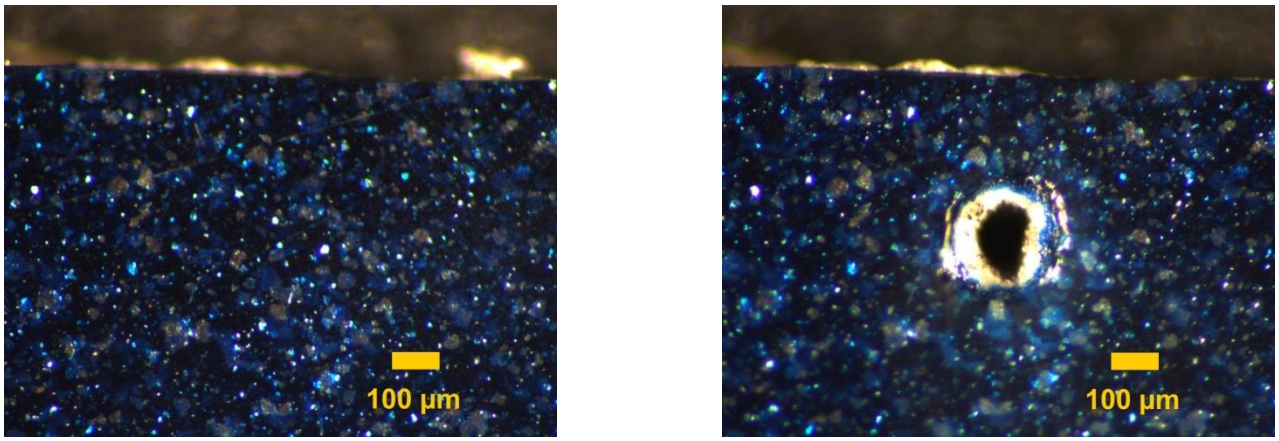

Figure 1: Car accident sample (car model: Renault Megane, collected 28.5.2019) top-view before (left) and after (right) a depth scan experiment, sample thickness is appr. 250 µm

The side-on view (Figure 2) shows the sequence of layers of the sample. On top there is a first dark layer of 40 to 50 µm thickness; the second layer appears whitish and is about 110 µm thick; the third layer again appears dark; and the fourth layer has a yellowish hue. Layers 3 and 4 are about 50 µm thick. The overall sample thickness is about 250 µm.

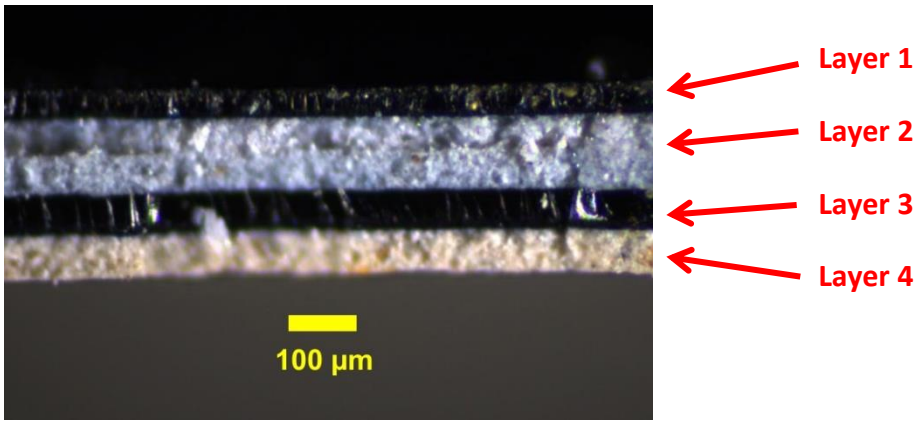

Figure 2: Breaking edge of a car paint sample seen from the side

Depth scan measurements were performed in the Raman-LIBS mode wherein the sample was measured at a single point or multiple points first with Raman and then with LIBS. After the LIBS measurement, the sample was moved upward to compensate for the loss of material before the next Raman measurement.

In the present case, a step size of 10 µm was chosen between two successive LIBS measurements. Since the ablation rate strongly depends on the material properties in the individual layers, it is highly probable that the amount of material removed per measurement varies significantly during one depth scan experiment.

For Raman measurements, a laser excitation wavelength of 532 nm was chosen. The laser power on the sample was 5 mW. The acquisition time per spectrum was 30 s. Horizontal binning of the detector camera was set to 4 pixels in order to improve the signal-to-noise ratio. The spectral resolution of the detector for Raman measurements was approximately 2.5 cm^{-1}.

For LIBS, a laser energy of 4 mJ per pulse was typically used. Three laser pulses were accumulated per LIBS spectrum. The temporal delay for starting signal acquisition after the laser pulse was set to 0.8 µs in order to effectively exclude the non-specific continuous background signal from the plasma plume. The spectral resolution of the LIBS arm of the spectrometer was in the range of 13 to 35 pm, depending on the wavelength between 190 and 520 nm.

The spectra were analyzed by assignment of the Raman bands to potential molecules, and the LIBS emission lines to elements. To visualize changes between spectra during the depth profile, LIBS line integrals as well as standard normal variates for the Raman and LIBS spectra were calculated. The standard normal variates were calculated (SNV) according to the following formula (adapted from [2]):

$$I_{SNV}(x) = \frac{I(x)-\mu}{\sigma} \qquad (1)$$

Here, $I_{SNV}(x)$ is the normalized intensity, I(x) is the raw intensity of a spectrum at point x, where x is the wavenumber in the case of Raman spectra and the wavelength in the case of LIBS spectra. Variables µ and σ are the average and standard deviations of the raw or background corrected intensity spectra, respectively, calculated over the entire spectral range. For background correction of Raman spectra, the method airPLS as described in [4] was used.

Results and Discussion

1.1 Raman spectra of single point depth scan

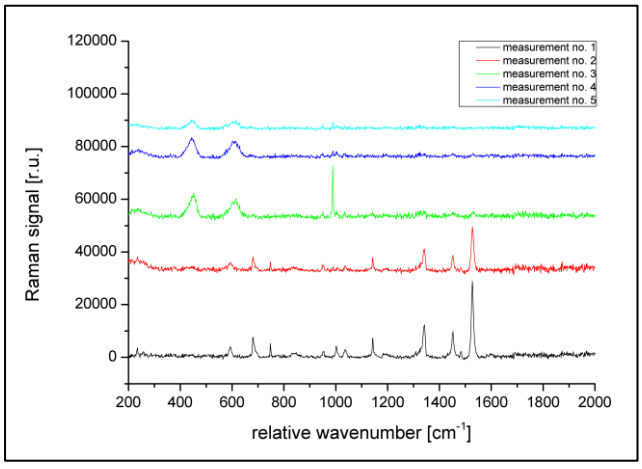

Figure 3: First five Raman spectra (background-corrected) from a single point depth scan experiment

First, depth scan experiments with 70 cycles of alternating Raman and LIBS measurements on a single point were performed. Exemplarily, Raman spectra of the first five measurements are shown in Figure 3. The first spectrum (black) is characterized by intense Raman bands at 1342 cm^{-1}, 1452 cm^{-1} and 1529 cm^{-1}. As already described in a previous Application Note, by comparing this spectrum with approximately 25,000 reference spectra of the KnowItAll® Raman Spectral Library (Bio-Rad Laboratories, Hercules, California, USA) these bands can be assigned to vibrations of copper-phthalocyanine (Cu-PC) which is the major pigment in this car paint sample. The Raman bands at 594 cm^{-1},

681 cm^{-1} and 748 cm^{-1} can also be assigned to vibrations of this pigment. Smaller Raman bands at 1002 cm^{-1} and 1036 cm^{-1} can be assigned to styrene also found in other car paint samples [5].

The bands assigned to phthalocyanine disappear after the second measurement while two broad bands at 452 cm^{-1} and 615 cm^{-1} appear. As previously shown, these bands can be assigned to vibrations from Rutile (TiO_2). One can conclude that the topmost layer of the sample is already ablated after the first two LIBS measurements thereby exposing the second layer for the following Raman measurement.

In order to give an overview of all 70 acquired Raman spectra, the standard normal variate (SNV) for every spectrum was calculated and plotted in Figure 4.

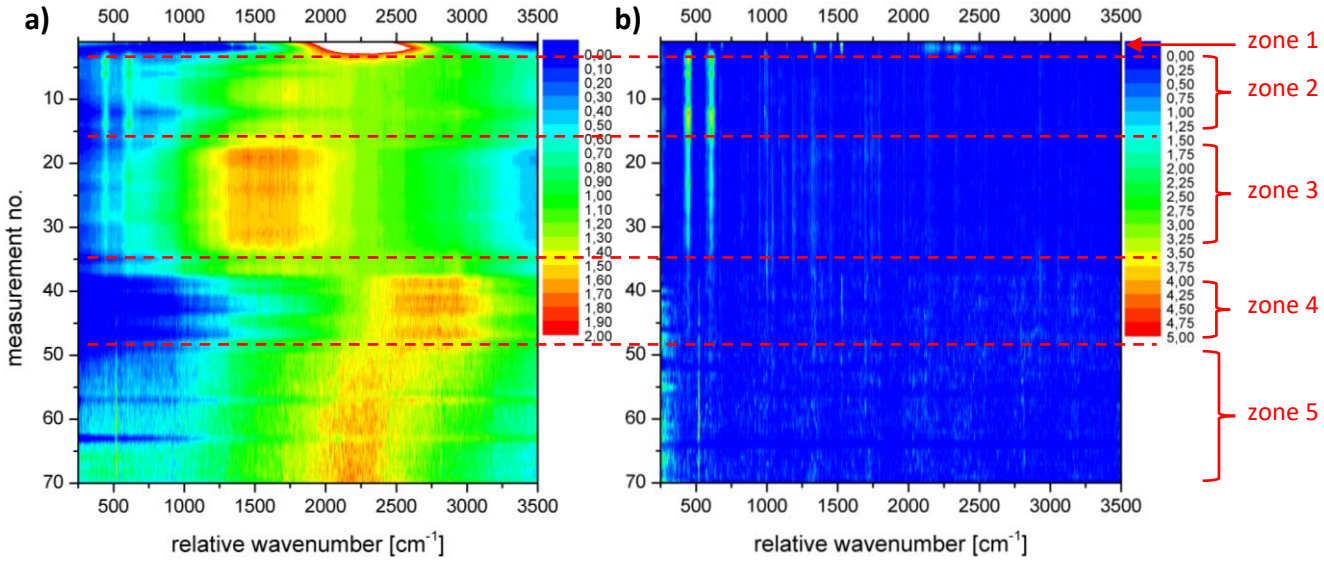

Figure 4: SNV-normalized Raman spectra; a) SNV of the raw spectra including fluorescence background; b) SNV of the background corrected spectra

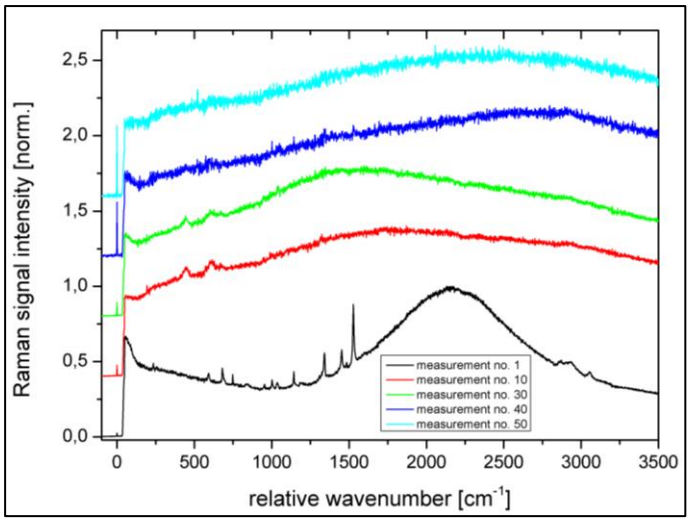

Figure 5: normalized raw spectra which are characteristic for the five different zones, for a better comparability of the spectra, a relative shift of 0.4 along the y-axis was applied

The SNV plot of the raw spectra including fluorescence background (Figure 4a) is dominated by the spectral position of the fluorescence bands. Five zones with different fluorescence patterns can be clearly distinguished. In Figure 4, the zones are marked with dashed lines. Figure 5 shows five characteristic Raman spectra of the five zones.

The spectrum of the topmost zone has a rather sharp and very intense fluorescence peak at ~ 2200 cm^{-1}. Also, three tiny maxima on the rising slope of the fluorescence band can be seen at 1340, 1450 and 1530 cm^{-1}. These Raman bands, like the two others at 600 and 680 cm^{-1} already known from Cu-PC, are even more visible in

Figure 4b where the background fluorescence was subtracted. The first zone is related to the first measurement (black curve in Figure 5).

The second zone belonging to measurements 3 to 15 has a rather broad fluorescence distribution peaking at ~ 1750 cm^{-1}. After subtraction of the fluorescence background, high SNV values can be observed at 452 and 615 cm^{-1} representing the two Raman bands assigned to TiO_2. In the third zone the fluorescence is further blue-shifted to 1500 cm^{-1} while the SNV values at 452 and 615 cm^{-1} representing the two Raman bands assigned to TiO_2 are still high. The third zone covers measurements 17 to 32. The red and green curves in Figure 5 are characteristic for zone 2 and 3, respectively.

A forth zone ranging from measurements 39 to 47 has a red-shifted fluorescence pattern with a maximum at around 2700 cm^{-1}. The TiO_2 peaks are no longer apparent. A Raman band at 521 cm^{-1}, assigned to silicon, begins to appear around measurement 45, which is more visible in the background-corrected SNV plot (Figure 4b). Also, the main Cu-PC Raman band at 1530 cm^{-1} arises again, although weakly.

For the fifth zone, starting at measurement 50, again a blue-shift in the fluorescence peak can be observed. The Raman band at 521 cm^{-1} assigned to silicon appears in the raw spectra as can be seen in the cyan-colored spectrum in Figure 5. Due to decreasing signal intensity, the relative noise in the spectra also increases. This is observable in Figure 5 as weak and randomly distributed local maxima in the background-corrected spectra.

From the micrograph in Figure 2, the actual coarse composition of the sample is known. It is therefore possible to derive a preliminary assignment of measurement zone to a sample layer:

zone 1:	layer 1 (characterized by the presence of pigment Cu-PC and the absence of TiO_2)
zones 2 and 3:	layer 2 (characterized by the presence of TiO_2)
zone 4:	layer 3 (characterized by the re-emergence of Cu-PC)
zone 5:	stepwise breakthrough through the sample (characterized by the increasing relative intensity of the silicon Raman band and noise)

Interestingly, layer 4 of the sample (see refer to Figure 2), which should be discernible by a re-emergence of TiO_2 Raman bands, could not be identified.

1.2 LIBS of single point depth scan

Alternating with Raman measurements, at each z-position one LIBS spectrum was obtained. The following graph shows the spectrum of the first measurement:

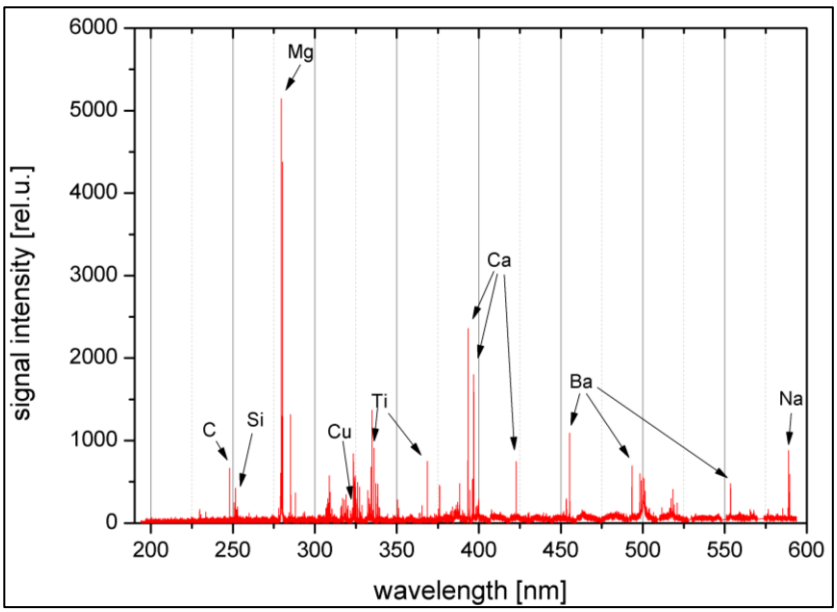

Figure 6: LIBS spectrum of the first measurement of the single point depth scan with peaks assignments

The most significant elements identified in the spectrum are indicated in Figure 6. Next, the dependence of the signal intensity for each element from the measurement number and hence from the depth of the hole drilled by the repeated laser shots was investigated.

For this purpose, two strong, self-absorption-free emission lines for each element were selected and integrated using the raw spectra. Afterwards the average of the two integrals was calculated. The values for silicon, barium and titanium are shown in Figure 7.

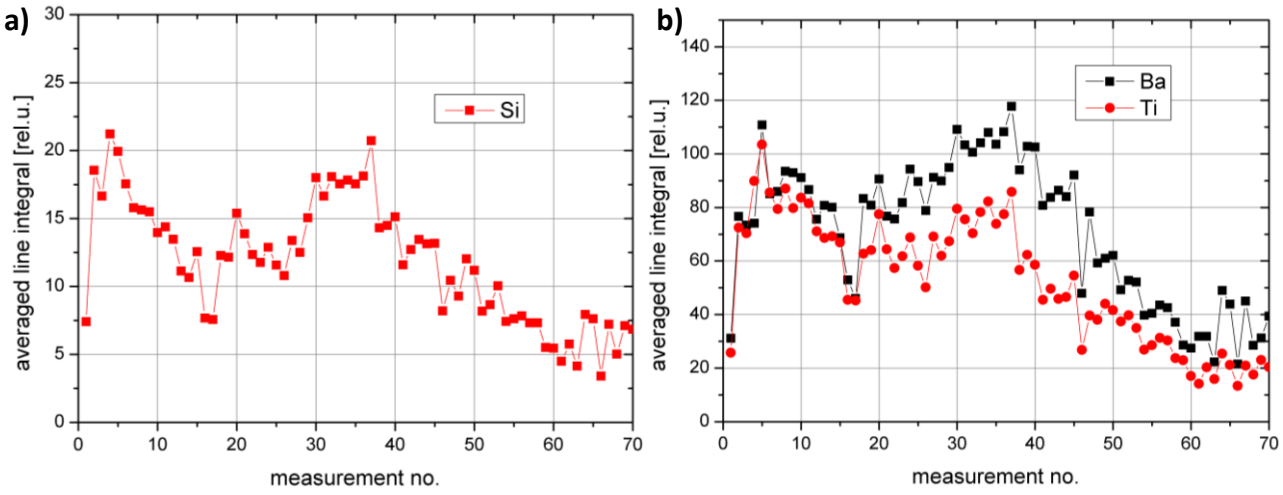

Figure 7: Average of the integral of two lines in the LIBS spectrum for a) the silicon lines and b) the barium and titanium lines over the measurement number

Surprisingly, no increase of the analyzed Si lines and no sharp signal loss for the other elements were observed at the point of sample breakthrough. Specially, Ba and Ti, which are used as fillers in plastics as sulfates and peroxides, show strong LIBS signals in the measured spectra and do not fade upon breakthrough. It could be assumed that due to the nearly cylindrical shape of the hole with a diameter of roughly 100 x 150 µm^2 and a final depth of 250 µm, the inner walls of the cylinder increasingly contribute to the LIBS signal upon growing depth resulting in a poor depth resolution.

In order to confirm this assumption, a second experiment was conducted. The area surrounding the drilled hole was removed at the rate of advancing depth using repetitive Raman-LIBS measurements in a 3 x 3 grid. The spectra at the center point (see chapter 2) were then analyzed for comparison.

2.1 Raman spectra of the central point in a 3 x 3 point depth scan

Figure 8 shows the sample surface before and after the measurement. The distance between the grid points (displayed as green circles in Figure 8a)) was 50 µm. The Raman spectra were acquired with 5 mW and an integration time of 15 s. For LIBS, the laser pulse energy was reduced from 4 mJ (used in the single point experiment) to 3 mJ per pulse while accumulating over three pulses.

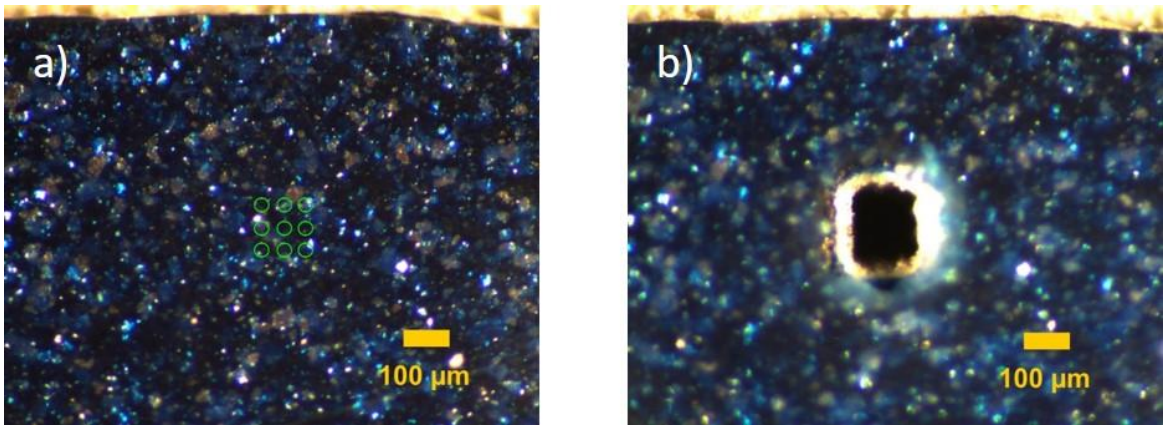

Figure 8: Sample a) before and b) after the 3x3 raster scan measurement, the raster points are marked in a) by green circles

Like the single point measurement, the Raman spectra were SNV normalized and the SNV values of the raw and the background corrected spectra were plotted. The results for the central sampling point are displayed in Figure 9.

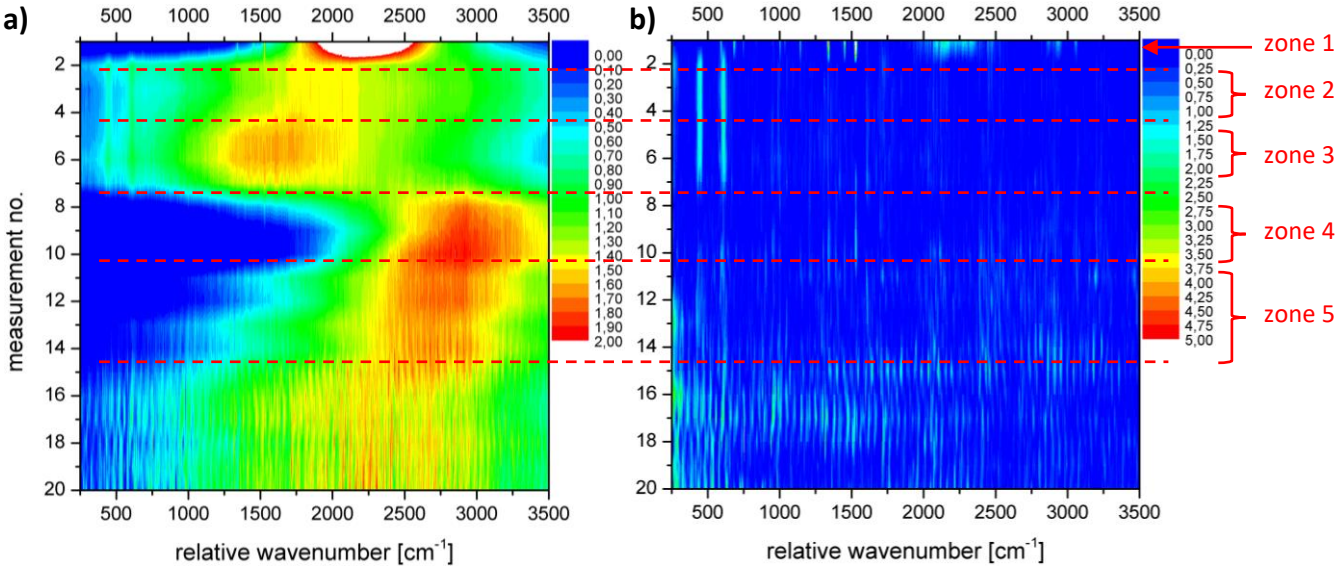

Figure 9: SNV values of Raman spectra of the central of 3 x 3 sampling points for a) the raw spectra and b) the background corrected spectra.

The patterns of the graphs are very similar to those of the single point measurement (compare Figure 9 and Figure 4). Again, the same five zones can be differentiated. Similarly to the single point measurement in zone 1 and measurements 9 and 10 in zone 4, high SNV values can be seen at 1342 cm^{-1}, 1452 cm^{-1} and

1529 cm^{-1} (Figure 9b). As described, those bands can be assigned to vibrations of Cu-PC. In zones 2 and 3, high SNV values are observed at 452 cm^{-1} and 615 cm^{-1}, which are attributable to vibrations of TiO_2. As indicated by the disappearance of these bands in Zone 3, layer 2 ends after measurement 7. In contrast to the single-point measurement, these vibrations reappear at measurement 10 at the border of zones 4 and 5. From this, and from the occurrence of Cu-PC bands, it can be concluded that zone 4 (layer 3) ends with measurement 10. More precisely, measurement 10 represents the transition to layer 4. After measurement 10, the signal-to-noise-ratio decreases significantly. From this, we can conclude that the crater is already close to the break-through point. This means that despite the lower laser pulse energy, there is a significantly higher ablation rate compared to the single-point experiment where the breakthrough was observed after 45 measurements.

2.2 LIBS spectra of the central point in a 3 x 3 point depth scan

Again, the line integrals of the analyzed elements were calculated from the LIBS spectra. The results for silicon, barium and titanium are shown in Figure 10.

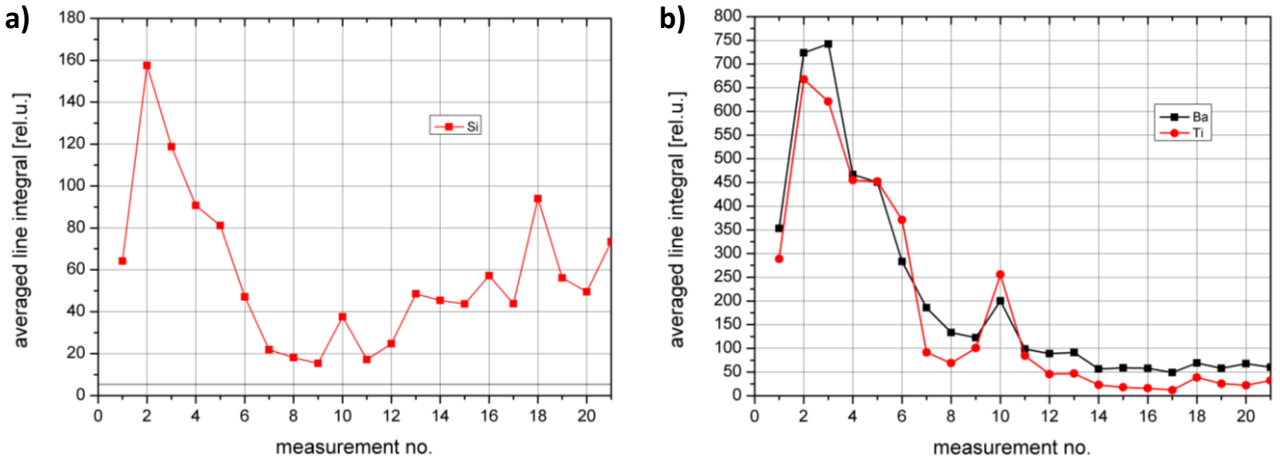

Figure 10: Averaged line integrals calculated using the LIBS spectra of the central point in the 3 x 3 point measurement of a) the silicon lines and b) the lines barium and titanium over the measurement number.

In contrast to the single point experiment, the averaged line integrals of the LIBS signals show dependencies on the measurement number, and thus, on the depth of the hole. For barium and titanium, two maxima can be seen: the first maximum at measurement 2 or 3 and the second at measurement 10 (Figure 10b). These elements are known to be part of filling materials in automotive paint coatings. Therefore, we assume that the high integral values arise from layers 2 and 4 (see Figure 2).

The averaged line integrals for silicon show a similar trend. They show a maximum at measurement 2 followed by a drop, and then a second maximum at measurement 10. In contrast to the barium and titanium results, a moderate but continuous increase in the integral of the silicon lines can be observed starting at measurement 12. This signal trend indicates the gradual perforation of the sample, and that the increasing Si signals come from the attached poly-crystalline silicon beneath.

Other detected elements also display a predictable trend through the course of sample drilling. The results for aluminum, calcium, magnesium and carbon are shown below in Figure 11. Aluminum has a maximum at measurement 1 (layer 1), whereas magnesium and calcium have their maxima at measurement no 2. For all

three elements, no second maximum in layer 3 was observed. Carbon has a maximum at measurement no. 6 followed by a continuous decrease of the averaged line integral.

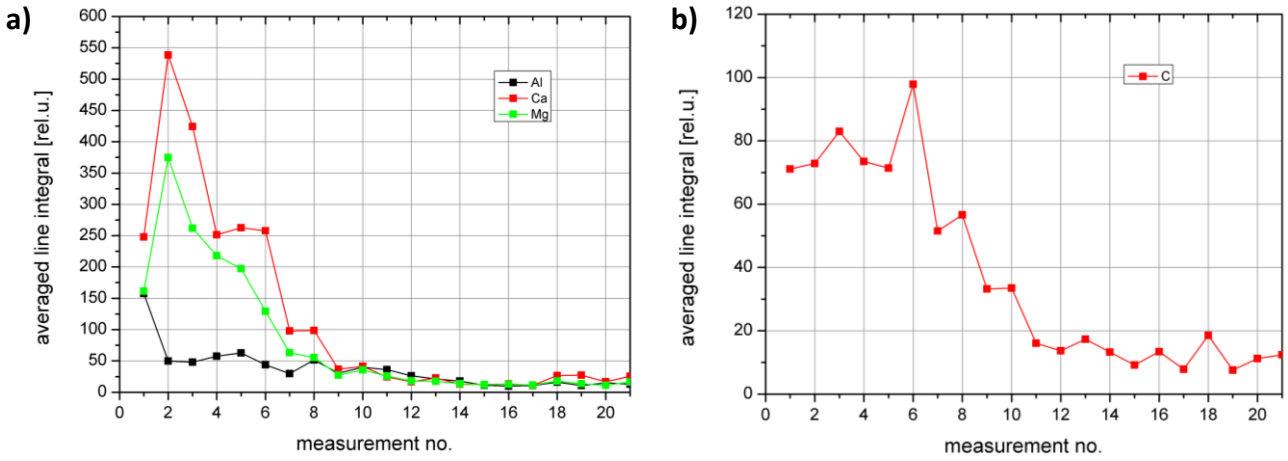

Figure 11: Averaged line integrals calculated using the LIBS spectra of the central point in the 3 x 3 point measurement for a) aluminum, calcium and magnesium and b) for carbon.

From these results we can conclude that, as opposed to a single point measurement, the modified 3 x 3 sampling method:

1. Yields actual depth related information of the elemental distribution.
2. Significantly increases the ablation rate, as indicated by the reduced number of laser pulses required to puncture the sample—12 rather that 45-50.

2.3 Combined analysis of Raman and LIBS spectra of the central point in a 3 x 3 point depth scan

A final point of interest is the conjunct evaluation of information obtained from both Raman and LIBS measurements. For this purpose, SNV normalization was applied to the LIBS spectra and graphs of spectral ranges which contain distinctive elemental lines were arranged with the SNV Raman spectra in one diagram.

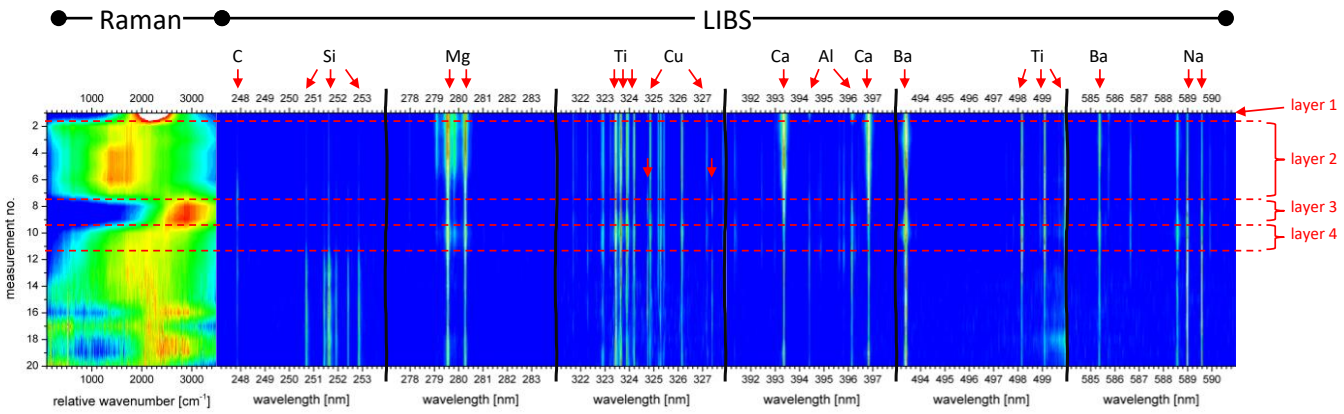

Figure 12: SNV values determined from the first 20 raw Raman spectra and selected parts of the LIBS spectra (each within a spectral window of 7 nm) of the central point in the 3 x 3 point experiment.

There are numerous correlations between the Raman/fluorescence and LIBS spectra which mutually support the analytical information obtained by each method for depth profiling of layered structures.

For the layer one measurement, high SNV values in the LIBS spectrum are observed for lines corresponding to magnesium (Mg: 279.553 and 280.270 nm), titanium (Ti: 323.4551 and 323.657 nm), calcium (Ca: 393,366. and 396.8847 nm), barium (Ba: 493.408 and 585.368 nm), aluminum (Al: 394.401 nm and 396.152 nm) and copper (Cu: 324.754 nm and 327.396 nm) (Figure 12). Corresponding Raman spectral bands attributable to copper-phthalocyanine and styrene are detected, as well as high fluorescence background around 2200 cm^{-1} (see Figure 1 and Figure 12). Obviously, the first Raman measurement, which occurred before the first LIBS measurement, measured the topmost layer of the sample as indicated by the presence of the pigment signal (Cu-PC), the matrix signal (styrene), and by the absence of the rutile (TiO_2) signal. Then, the first 3-pulse LIBS measurement ablates layer one completely and reaches layer two, as indicated by the presence of Ti and Ba signals.

The second layer, (measurements 2 through 7) is characterized by immediately declining signal intensities for Cu and Al lines, and strong line intensities of Ti, Ba, Mg and Ca. The Raman spectra measured in this layer also show a clear and immediate decrease in the signal intensity of the bands assigned to Cu-PC and arising bands that can be assigned to TiO_2. Furthermore, the maximum of the fluorescence background shifts to ~1750 cm^{-1}, also indicating a change in chemical composition of the analyzed material.

In layer 3 (measurements 8 and 9) the sample fluorescence is once again strongly shifted, now towards longer wavelengths. In the Raman spectra, bands assigned to copper-phthalocyanine arise, a trend corroborated by the presence of copper identified by LIBS (see red arrows inside the diagram of Figure 12). The rise of the Cu signal is accompanied by a temporary drop of the Ti, Ba and Mg signals.

Measurements 10 (as transition) and 11 belong to Layer 4. The background fluorescence is shifted back towards shorter wavelengths. In the Raman spectra, weak bands related to Rutile appear again, while in the LIBS spectra, the signals of Ti, Ba and Mg become stronger.

The point of sample breakthrough is clearly indicated by the signal course of silicon in both Raman and LIBS results. Within the Raman spectra, the emerging Si band at 521 cm^{-1} is a clear indicator, while in the normalized LIBS spectra, the relative intensity increase of the Si lines around 251.5 nm is apparent. Although (as seen in Figure 10a) Si has good signal intensity from the first measurement, its relative contribution to the overall signal sharply increases with measurement 12.

Finally, C and Na behave differently than all other elements present in the sample. Na (588.998 and 589.592 nm) has rather stable signals in the SNV-normalized data throughout the entire measurement range. C (247.856 nm) is relatively weak in the first 5 measurements and reaches maximum intensity in measurement 6. Later, it maintains a smaller but clearly visible proportion among the remaining elemental lines.

Conclusion

It was shown that the Coralis instrument can be used to obtain detailed information about the depth profiles of automotive paint samples with thicknesses of more than a hundred microns. Depending on the sample properties, it may be advisable to adjust the experimental conditions for meaningful results. In the

presented case, when drilling a hole at a single sample point, only Raman spectra produced depth-resolved results. Due to an unfavorable ratio of crater diameter and depth, the LIBS plasma plume continuously ablated material from the walls of the developing crater, blurring the depth dependence of the individual elements.

By also ablating the immediate surrounding area of the desired sample point, as done in the 3 by 3 measurement, LIBS produces information indicating the distribution of different elements depending on the depth. However, even in this arrangement, there is still a minor contribution from the inner walls of the developing crater. This can be seen by the not completely disappearing signals of most of the detectable elements. In all cases, placing the sample on a substrate whose Raman and LIBS spectra explicitly differs from that of the sample (e.g. on poly-crystalline silicon) enables the clear detection of sample breakthrough.

The combination of Raman and LIBS indeed enables a chemical depth profiling of automotive paint samples. It is also important to emphasize that the fluorescence background measured simultaneously with the Raman spectra gives valuable information and supports the characterization and differentiation of automotive paint. As shown, the Raman spectra yield characteristic spectra for every sample layer. The built-in database, the KnowItAll® Raman Spectral Library, and analysis using Bio-Rad's software KnowItAll® Raman Identification Pro[1] enable the detailed analysis of materials and pigments.

The elemental distribution revealed by LIBS may give additional information about materials not visible with Raman, or about trace elements or impurities which may be characteristic for samples of different manufacturers.

The presentation of the SNV-normalized data in a pseudo color image as shown above is an interesting method of visualizing these data. At a glance, an entire set of spectra with largely differing intensities can be displayed, while significant changes between the spectra attributed to different sample zones become obvious. This kind of data presentation will be further tested in studies comparing depth profiles of various different samples.

References

[1] Balzer H, Hoehne M, Noll R, Strum V. New approach to online monitoring of the Al depth profile of the hot-dip galvanised sheet steel using LIBS. Anal Bioanal Chem (2006) 385: 225–233

[2] Syvilay D, Wilkie-Chancellier N, Tricherau B, Texier A, Martinez A, Serfaty S, Detalle V. Evaluation of the standard normal variate method for Laser-Induced Breakdown Spectroscopy data treatment applied to the discrimination of painting layers. Spectrochim. Acta Part B 114 (2015): 38–45.

[3] Glaus R, Hahn DW. Fiber-coupled laser-induced breakdown and Raman spectroscopy for flexible sample characterization with depth profiling capabilities. Spectrochim. Acta Part B 100 (2014): 116–122.

[4] Zhang ZM, Chen S, Liang YZ. Baseline correction using adaptive iteratively reweighted penalized least squares. *Analyst*, *135*(5) (2010): 1138-1146.

[5] Ferreira, KB, Oliveira AGG, Gomes JA. Raman spectroscopy of automotive paints: Forensic analysis of variability and spectral quality. Spectrosc. Lett. 50 (2017): 102-110.

[1] KnowItAll is a trademark of Bio-Rad Laboratories, Inc. in certain jurisdictions